

EPSDIC-2016



ISSN: 2321-7758

VIBRATIONAL AND UV/VIS SPECTROSCOPIC, NBO ANALYSIS OF 6-(Y,Y-DIMETHYLALLYLAMINO) PURINE BY AB INITIO D CALCULATIONS

A.VEERAAH, M.SATYAVANI & KATTAESWARSRIKANTH

Molecular spectroscopy laboratory, Department of Physics, D.N.R.College(A), Bhimavaram, A.P., India-534 202

ABSTRACT

6-(Y,Y-Dimethylallylamino)purine (6DMP) is a bacteria-derived ribosidecytokinin used to grow plant tissues such as tobacco and soybean callus. 6DMP is a precursor of the cytokinin Zeatin. It has been used in Schenk and Hidebrandt medium to support in Vitro propagation of micro shoot cultures from shoot tips of Genistaplants. The vibrational and electronic properties of 6-(Y,Y-Dimethylallylamino) have been studied in the ground state using density functional theory (D) employing B3LYP exchange correlation with the 6-31G(d, p) basis set. Optimized parameters, vibrational frequencies, some important properties, excited states etc., of the compound were calculated and presented. The complete assignments of fundamental modes were performed on the basis of the potential energy distribution (PED). UV-visible spectrum of the compound was predicted theoretically using SAC-CI method and presented. These studies proved that the compound can be used as one of the potential light sources in the UV region. Thermodynamic properties, Mulliken and natural atomic charge distribution were calculated using both Hatree-Fock and Density Functional method. ¹H and ¹³c NMR chemical shifts of the molecule were calculated using gauge including atomic orbital method. Stability of the molecule arising from hyperconjugative interactions and charge delocalization has been analyzed using natural bond analysis. The first order hyperpolarizability (β) and molecular electrostatic potential of the molecule were also computed and the respective electrophilic and nucleophilic attacking centres are identified and presented. The electron density based local reactivity descriptor such as Fukui functions were calculated to explain the chemically reactive site in the molecule.

Keywords: 6-(Y,Y-Dimethylallylamino), D, SAC-CI, HOMO-LUMO and NBO

1. Introduction:

The purine and its derivatives are the most important class of organic compounds containing two condensed heterocyclic rings. Purine ring system is important because some of its derivatives in particular adenine and guanine are the building blocks of RNA and DNA. A 1.3g urine molecule contains both a pyrimidine ring and an imidazole ring. Purine exists in two tautomeric forms. Consideration of these factors influenced to undertake spectroscopic study of the title compound [1, 2, 3]. Purine is one of the purine base series, several molecules of which are components of nucleic acids. IR and Raman spectra for Purine and its deuterated derivatives have been investigated previously, and assignments for a number of bands have been proposed. Argon matrix IR spectra have also been reported and interpreted as corresponding to two tautomeric forms of purine where the proton is attached to either the N₇ and N₉ atoms. Assignments for the observed bands have also been proposed from a normal coordinate analysis carried out using an empirical force field [4]. The vibrational spectra of purine have been investigated by IR and Raman spectroscopy [5,6] and argon matrix IR

spectroscopy[7]. We give here resonance Raman(RR) spectra for purine in aqueous solution obtained with excitation at 280, 257 and 222nm. Relative to the -R spectra obtained with excitation at 1064nm, a considerable change in intensity is observed for several bands. As with imidazole [8], adenine and guanine residues[9], these band are expected to correspond to totally symmetric in-plane normal modes involving, in particular, the stretching of those ring bonds which are perturbed in the excited state relative to the ground state. 6-Benzylaminopurine (Bap) derivatives represent heterocyclic compounds showing a large scale of biological activities. As the plant growth hormones, called Cytokinins, they have been intensively studied since the 1960s. The key role of the cytokinnis lies principally in participation in the controlling of the processes related to the plant cell division and senescence[11-14].



Fig.1: Optimized Molecular structure of 6-(Y,Y-Dimethylallylamino)purine along with numbering of atom.

However, literature survey indicates that there are limited investigations on the vibrational spectra of 6-(Y,Y-Dimethylallylamino)purine and its derivatives so far. Hence, in this study, we report the vibrational and UV-Visible spectra, NBO analysis, HOMO-LUMO studies on 6-(Y,Y-Dimethylallylamino)purine (herea er it is termed as 6DMP) using D calculations for the first time.

2. Computational Details:

As a first step, the most optimized structural parameters, energy and vibrational frequencies of the molecule have been calculated by using B3[15] exchange functional combined with the LYP [16] correlation functional resulting in the B3LYP density functional method at 6-31G(d, p) basis sets. All the computations were performed using Gaussian 09W program[17] and visualized using Gauss-View molecular visualization program package[18] and Chemcra molecular visulisation program[19] packages on an i5 processor. At the optimized structure of the 6DMP, no imaginary frequencies were obtained, proving that a true minimum on the potential energy surface was found. The optimum geometry was determined by minimizing the energy with respect to all geometrical parameters without imposing molecular symmetry constraints. The cartesian representation of the force constants were transferred to a non-redundant set of local symmetry coordinates, chosen in accordance to the recommendations of Pulay et al [20, 21]. The NBO calculations[22]were performed using NBO 3.1 program available in the Gaussian 09W package at the D /B3LYP level to understand the intra-molecular delocalization or hyper conjugation. UV-Vis spectrum is predicted using TD D calculations supplementing with 6-31G(d, p) basis set.

3. Results and Discussion

3.1. Molecular geometry

The most optimized structural parameters of 6DMPwere calculated by D /B3LYP level with 6-31 G (d, p) basis set are presented in table as shown in below in Table 1.

Table 1: Optimized geometrical parameters of 6-(Y,Y-Dimethylallylamino)purine (6DMP) obtained by B3LYP/6-31G(d,p) density functional calculations

Bond length ^a (6-31G(d,p)) Å ^o		Bond Angle ^a (6-31G(d,p)) Value(°)		Bond Angle ^a (6-31G(d,p)) Value(°)	
C1-N2	1.353	C1-N2-C3	119.2	C12-C11-H21	110.5
N2-C3	1.337	N2-C3-N4	128.8	C11-C12-H22	113.8
C3-N4	1.337	C3-N4-C5	110.7	C13-C12-H22	118.0
N4-C5	1.337	N4-C5-C6	127.6	C13-C14-H23	113.6
C5-C6	1.403	C5-C6-C1	115.4	C13-C14-H24	110.5
C6-C1	1.418	C6-C1-N2	118.0	C13-C14-H25	110.4
C6-N7	1.389	C6-N7-C8	104.4	C13-C15-H26	111.9
N7-C8	1.309	N7-C8-N9	113.2	C13-C15-H27	110.9
C8-N9	1.376	C8-N9-C5	106.8	C13-C15-H28	111.0
N9-C5	1.377	N9-C5-C6	104.7	H24-C14-H25	106.3
C1-N10	1.353	C6-C1-N10	125.8	H23-C14-H24	107.6
N10-C11	1.462	N2-C1-N10	116.0	H23-C14-H25	107.9
C11-C12	1.505	C1-N10-C11	128.0	H26-C15-H27	108.2
C12-C13	1.342	N10-C11-C12	110.5	H27-C15-H28	106.3
C13-C14	1.509	C11-C12-C13	128.0	H26-C15-H28	108.0
C13-C15	1.509	C12-C13-C14	125.1		
C3-H16	1.088	C12-C13-C15	120.4		
N9-H18	1.008	C14-C13-C15	114.3		
C8-H17	1.081	N2-C3-H16	115.2		
N10-H19	1.011	N4-C3-H16	115.8		
C11-H20	1.096	C5-N9-H18	125.4		
C11-H21	1.093	C8-N9-H18	127.6		
C12-H22	1.089	N9-C8-H17	121.6		
C14-H23	1.091	N7-C8-H17	125.1		
C14-H24	1.097	C1-N10-H19	113.7		
C14-H25	1.097	C11-N10-H19	118.1		
C15-H26	1.093	N10-C11-H21	107.3		
C15-H27	1.097	N10-C11-H20	109.8		
C15-H28	1.097	C12-C11-H20	111.6		

The atom numbering scheme given in Fig.1. The calculated molecular structure for this compound is found to be non-planar and is as shown in Fig.1. In order to reveal all possible conformations of 6DMP, a detailed potential energy surface (PES) scan for C11-C12-C13-C14 dihedral angle was performed. The scan was carried out by

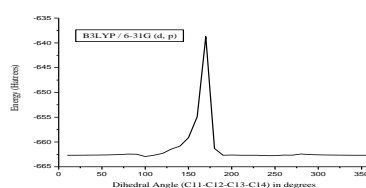


Fig.2: Potential energy surface scan for dihedral angle C11-C12-C13-C14 of 6-(Y,Y-Dimethylallylamino)purine

^aFor numbering of atoms refer to Fig. 1. Minimizing the potential energy in all geometrical parameters by changing the torsion angle every 10° for 360° rotation around the bond using 6-31G(d,p) basis set. The shape of the potential energy as a function of the dihedral angle is illustrated in Fig.2. The total minimum energy obtained by the D for the 6DMP was found to be -662.686214 Hartrees. The order of the theoretical bond angles are $N2-C3-N4 > C1-N10-C11 > C11-C12-C13 > C8-N9-H18 > N4-C5-C6$.

3.2. Vibrational analysis:

The maximum number of potentially active observable fundamentals of a non-linear molecule, which contains N atoms, is equal to $(3N - 6)$ apart from three translational and three rotational degrees of freedom [23, 24]. Hence, 6DMP molecule has 28 atoms with 78 normal modes of vibrations and considered under C_1 point group symmetry. A detailed vibrational description can be given by normal coordinate analysis. The specific assignment to each frequency is attempted through Potential Energy Distribution (PED) method. For this purpose, the full set of defined internal coordinates is given in Table 2. To obtain the normal modes in a molecular coordinate system, local symmetry coordinates for 6DMP were recommended by Fogarasi and Pulay [25] and were presented in Table 3. This method is also useful for determining the mixing of other modes. But mostly the maximum contribution is agreed to be the most significant mode.

Table 2: Definition of internal coordinates of 6-(Y,Y-Dimethylallylamino)purine (6DMP)

No.(i)	Symbol	Type	Definition ^a
Stretching			
1 to 3	R_i	CH	C3-H16, N9-H18, C8-H17
4-5	R_i	CC	C5-C6, C6-C1
6-9	R_i	CN(Ring1)	C1-N2, N2-C3, C3-N4, N4-C5,
10-13	R_i	CN(Ring2)	C6-N7, N7-C8, C8-N9, N9-C5
14	R_i	NH	N10-H19
15-23	R_i	CHsub	C11-H20, C11-H21, C12-H22, C14-H23, C14-24, C14-H25, C15-H26, C15-H27, C15-H28
24-27	R_i	CCsub	C11-C12, C12-C13, C13-C14, C13-C15
28-29	R_i	CN SUB	C1-N10, C11-N10
In-Plane bending			
30-37	γ_i	CCH	C5-N9-H18, C8-N9-H18, N9-C8-H17, N7-C8-H17, N2-C3-H16, N4-C3-H16, C13-C12-H22, C11-C12-H22
38-43	γ_i	Ring1	C1-N2-C3, N2-C3-N4, C3-N4-C5, N4-C5-N6, C5-N6-C1, C6-C1-N2
44-48	γ_i	Ring2	C5-C6-N7, C6-N7-C8, N7-C8-N9, C8-N9-C5, N9-C5-C6
49-50	γ_i	CCN	N2-C1-N10, C6-C1-N10
51-56	γ_i	CCC	C14-C13-C12, C15-C13-C12, C15-C13-C14, C12-C13-C14, C12-C13-C15, C14-C13-C15
57-61	γ_i	CCCSUB	C1-N10-C11, N10-C11-C12, C11-C12-C13.
62-63	γ_i	CCH(sub)	C12-C11-H20, C12-C11-H21,
64-65	γ_i	NCH	N10-C11-H20, N10-C11-H21
66-71	γ_i	CCH(MET)	C13-C14-H23, C13-C14-H24, C13-C14-H25,
72-77	γ_i	HCH	C13-C15-H26, C13-C15-H27, C13-C15-H28
			H23-C14-H24, H24-C14-H25, H23-C14-H25,

			H26-C15-H27, H27-C15-H28, H26-C15-H28
Out-of-plane bending			
78-81	ρ_i	CH	H16-C3-N2-N4, H18-N9-C5-C8, H17-C8-N9-N7, H22-C12-C11-C13
82	ρ_i	CN	N10-C1-C6-N2,
83-85	ρ_i	CC	C12-C13-C14-C15, C15-C13-C14-C12, C14-C13-C15-C12
86	ρ_i	NH	H19-N10-C11-C1
Torsion			
87-92	τ_i	RING 1	C1-C2-C3-C4, C2-C3-C4-C5, C3-C4-C5-C6, C4-C5-C6-C1, C5-C6-C1-C2, C6-C1-C2-C3
93-97	τ_i	RING2	C6-C7-C8-O9, C7-C8-O9-C5, C8-O9-C5-C6, O9-C5-C6-C7, C5-C6-C7-C8
98-99	τ_i	CCH3	(C12-C15)-C13-C14-(H23-H24-H25), (C12-C14)-C13-C15-(H26-H27-H28)
100-101	τ_i	Butterfly	N9-C5-C6-C1, N4-C5-C6-N7

^aFor numbering of atom refer Fig.1

Table 3: Definition of local-symmetry coordinates 6-(Y,Y-Dimethylallylamino)purine (6DMP)

No.(i)	Symbol	Definition
Stretching		
1 to 3	$\nu(\text{C-H})$	R1, R2, R3
4-5	$\nu(\text{C-C})\text{AR}$	R4, R5
6-13	$\nu(\text{C-N})$	R6, R7, R8, R9, R10, R11, R12, R13
14	$\nu(\text{N-H})$	R14
15	$\nu\text{CH}_2\text{SS}$	$(\text{R15}+\text{R16})/\sqrt{2}$
16	$\nu\text{CH}_2\text{AS}$	$(\text{R15}-\text{R16})/\sqrt{2}$
17-18	$\nu(\text{CH}_3)\text{SS}$	$(\text{R17}+\text{R18}+\text{R19})/\sqrt{2}, (\text{R20}+\text{R21}+\text{R22})/\sqrt{2}$
19-20	$\nu(\text{CH}_3)\text{IPS}$	$(2\text{R17}-\text{R18}-\text{R19})/\sqrt{6}, (2\text{R20}-\text{R21}-\text{R22})/\sqrt{6}$
21-22	$\nu(\text{CH}_3)\text{OPS}$	$(\text{R18}-\text{R19})/\sqrt{2}, (\text{R21}-\text{R22})/\sqrt{2}$
23	$\nu(\text{C-H})$	R23
24-27	$\nu(\text{C-C})\text{SUB}$	R24, R25, R26, R27
28-29	$\nu(\text{C-N})\text{SUB}$	R28, R29

In-Plane bending

30-33	β_{C-H}	$(\gamma_{30}-\gamma_{31})/\sqrt{2}, (\gamma_{32}-\gamma_{33})/\sqrt{2}, (\gamma_{34}-\gamma_{35})/\sqrt{2},$ $36-\gamma_{37})/\sqrt{2}.$	(γ
34	β_{Rtri}	$(\gamma_{38}-\gamma_{39}+\gamma_{40}-\gamma_{41}+\gamma_{42}-\gamma_{43})/\sqrt{6}.$	
35-36	β_{Rasy}	$(2\gamma_{38}-\gamma_{39}-\gamma_{40}+2\gamma_{41}-\gamma_{42}-\gamma_{43})/\sqrt{12},$ $(a-b)(\gamma_{45}-\gamma_{48})+(a+b)(\gamma_{46}-\gamma_{47})$	
37-38	β_{Rsym}	$(\gamma_{39}-\gamma_{40}+\gamma_{42}-\gamma_{43})/2,$ $\gamma_{44}+a(\gamma_{45}+\gamma_{48})-b(\gamma_{46}+\gamma_{47})$	
39	β_{C-N}	$(\gamma_{49}-\gamma_{50})/\sqrt{2}$	
40-42	β_{C-C}	$(\gamma_{51}-\gamma_{52})/\sqrt{2}, (\gamma_{53}-\gamma_{54})/\sqrt{2}, (\gamma_{55}-\gamma_{56})/\sqrt{2}$	
43-47	$\beta_{C-C_{SUB}}$	$\gamma_{57}, \gamma_{58}, \gamma_{59}, \gamma_{60}, \gamma_{61}$	
48	β_{CH_2sc}	$(\gamma_{62}+\gamma_{64}+\gamma_{63}+\gamma_{65})/2$	
49	β_{CH_2ro}	$(\gamma_{62}+\gamma_{64}-\gamma_{63}-\gamma_{65})/2$	
50	β_{CH_2wa}	$(\gamma_{62}-\gamma_{64}+\gamma_{63}-\gamma_{65})/2$	
51	β_{CH_2tw}	$(\gamma_{62}-\gamma_{64}-\gamma_{63}+\gamma_{65})/2$	
52-53	β_{CH_3sb}	$(-\gamma_{66}-\gamma_{67}-\gamma_{68}+\gamma_{69}+\gamma_{70}+\gamma_{71})/\sqrt{6},$ $(-\gamma_{72}-\gamma_{73}-\gamma_{74}+\gamma_{75}+\gamma_{76}+\gamma_{77})/\sqrt{6}$	
54-55	β_{CH_3ipb}	$(-\gamma_{69}-\gamma_{70}-2\gamma_{71})/\sqrt{6}, (-\gamma_{75}-\gamma_{76}-2\gamma_{77})/\sqrt{6}$	
56-57	β_{CH_3opb}	$(\gamma_{69}-\gamma_{70})\sqrt{2}, (\gamma_{75}-\gamma_{76})\sqrt{2}$	
58-59	β_{CH_3ipr}	$(2\gamma_{66}-\gamma_{67}-\gamma_{68})/\sqrt{6}, (2\gamma_{72}-\gamma_{73}-\gamma_{74})/\sqrt{6}$	
60-61	β_{CH_3opr}	$(\gamma_{66}-\gamma_{67})/\sqrt{2}, (\gamma_{72}-\gamma_{73})/\sqrt{2}$	

Out of plane bending

62-64	ω_{C-H}	$\rho_{78}, \rho_{79}, \rho_{80}, \rho_{81}$
65	ω_{C-N}	ρ_{82}
66-68	ω_{C-C}	$\rho_{83}, \rho_{84}, \rho_{85}$
69	ω_{N-H}	ρ_{86}

Torsions

70	τ_{Rtri}	$(\tau_{87}-\tau_{88}+\tau_{89}-\tau_{90}+\tau_{91}-\tau_{92})/\sqrt{6}.$
71-72	τ_{Rasy}	$(\tau_{87}-\tau_{89}+\tau_{90}-\tau_{92})/2,$ $b(\tau_{93}+\tau_{97})+a(\tau_{94}+\tau_{96})+\tau_{95}$

73-74	τ_{Rsym}	$(-\tau_{87}-2\tau_{88}-\tau_{89}+\tau_{90}+2\tau_{91}-\tau_{92})/\sqrt{12}$ $(a-b)(\tau_{96}-\tau_{94})+(1-a)(\tau_{97}-\tau_{93})$
76-77	τ_{CCH_3}	τ_{98}, τ_{99}
78	Butter	$(\tau_{100}-\tau_{101})/2$

Where $a=\cos 144^\circ$, $b=\cos 72^\circ$.

Abbreviations: ν , stretching; β , in plane bending; ω , out of plane bending; τ , torsion, *ss*, symmetrical stretching, *ass*, asymmetrical stretching, *sc*, scissoring, *wa*, wagging, *tw*, twisting, *ro*, rocking, *tri*, trigonal deformation, *sym*, symmetrical deformation, *asy*, asymmetric deformation, *butter*, butterfly, *ar*, aromatic, *sub*, substitution.

^a The internal coordinates used here are defined in table given in Table 2

3.2.1. IR and Raman spectra:

The calculated IR and Raman Spectra are presented in Figures 3&4. Raman spectrum was plotted against Raman intensity Vs wavenumber and IR spectrum was plotted IR intensity Vs Wavenumber.

3.2.1.1. C-H vibrations:

The pure C-H stretching vibrations of aromatic and hetero aromatic compounds generally occur in the characteristic region $3100-3000\text{ cm}^{-1}$. While the wavenumbers for several of these are strongly implied by the recorded spectra, it is difficult to fully assign the CH stretching vibrations since some of the observed bands are undoubtedly due to, or perturbed by, combination bands from the lower frequency fundamentals ($\nu < 1600\text{ cm}^{-1}$). But theoretically we observed at 3174 cm^{-1} .

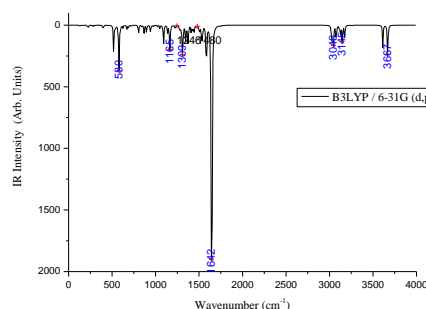


Fig. 3: Theoretical IR spectrum of 6-(Y,Y-Dimethylallylamino)purine

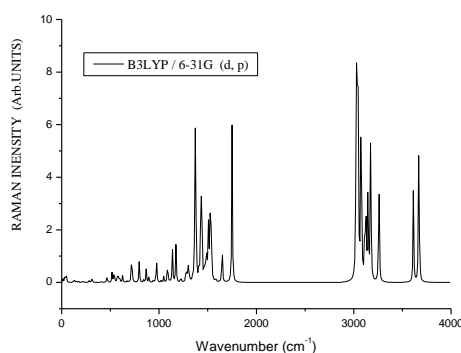


Fig. 4: Theoretical Raman spectrum of 6-(Y,Y-Dimethylallylamino)purine

3.2.1.2. CH3 vibrations:

For the assignments of CH₃ group frequencies, basically nine fundamentals can be associated to each CH₃ group namely, CH₃ss: symmetric stretch; CH₃ips: in-plane stretch (i.e., in-plane hydrogen stretching modes); CH₃ipb: in-plane-bending (i.e., hydrogen deformation modes); CH₃sb: symmetric bending; CH₃ipr: in-

plane rocking; CH₃ opr: out-of-plane rocking and tCH₃: twisting hydrogen bending modes. In addition to that, CH₃ops: out-of-plane stretch and CH₃opb: out-of-plane bending modes of the CH₃ group would be expected to be depolarized for A"symmetry species. The Raman and infrared bands associated with the CH₃ stretch groups were predicted at 302 to 3072.059 cm⁻¹.

3.2.1.3. CH₂ Vibrations:

The asymmetric CH₂ stretching vibration generally observed in the region 3000–2900cm⁻¹, while the CH₂ symmetric stretch will appear between 2900 and 2800cm⁻¹. The strong band observed at 3005cm⁻¹ in the IR spectrum is assigned to ν_{CH₂} asymmetric stretching which is not observed in the Raman spectrum. The band observed at 2956(vs)cm⁻¹ in the -IR spectrum and the band observed at 2955(ms)cm⁻¹ in the -Raman spectrum are assigned to ν_{CH₂} symmetric stretching. The scissoring vibrations are expected in the region 1455–1380cm⁻¹ and consist of medium intense bands. The twisting and rocking vibrations of CH₂ group are observed at 1148cm⁻¹ and 830cm⁻¹ in Raman spectrum respectively. The band observed at 1385cm⁻¹ in the IR spectrum is assigned to β_{CH₂} scissoring vibration which is not observed on the Raman spectrum. The band observed at 1195cm⁻¹ in the Raman spectrum is assigned to ω_{CH₂} wagging vibrations which is not observed in the IR spectrum.

3.2.1.4. N-H vibrations:

It is noted that the N-H stretching vibrations occur in the region 3600 cm⁻¹, but theoretically we observed at 3650 cm⁻¹

3.2.1.5. C-C vibrations:

In general, the bands around 1650 to 650cm⁻¹ in benzene are assigned to skeletal C-C stretching modes but we observed theoretically 1670 to 1680 cm⁻¹.

3.2.1.6. Ring Vibrations:

Several ring modes are affected by the substitution to the aromatic ring of 6DMP in the present study we observed the values at 224.746cm⁻¹, 280.85cm⁻¹, 298.67cm⁻¹, 395.76cm⁻¹, 538.94cm⁻¹, 569.58cm⁻¹, 578.94cm⁻¹, 593.56cm⁻¹, 625.79cm⁻¹, 686.00cm⁻¹, 718.96cm⁻¹, 896.20cm⁻¹, 942.47cm⁻¹, 1162.57cm⁻¹, 1173.64cm⁻¹ respectively

3.2.1.7. C-N Vibrations:

The identification of C-N and C=N vibrations is a very difficult task, since the mixing of several bands are possible in this region. However, With the help of animation we observed at 1350 and 1343 cm⁻¹

4. NBO analysis:

NBO analysis provides the most accurate possible 'natural Lewis structure' picture of ϕ , because all orbital details are mathematically chosen to include the highest possible percentage of the electron density. A useful aspect of the NBO method is that it gives information about interactions in both filled and virtual orbital spaces that could enhance the analysis of intra- and intermolecular interactions. It also provides a convenient basis for investigating charge transfer or conjugative

Table4: Second order perturbation theory analysis of fock matrix in NBO basis for 6-(Y,Y-Dimethylallyl amino) purine.

Donor(i)	Type	Ed/e	Acceptor(j)	Type	Ed/e	E(2)	E(i)-E(j)	f(i,j)
C1-N2	σ	1.98209	C6-N7	σ*	1.97603	3.80	1.28	0.062
C1-N2	σ	1.71529	C3-N4	σ*	1.98341	35.88	0.30	0.094
			C5-C6	σ*	1.97113	9.09	0.32	0.050
C1-C6	σ	1.97616	C5-C6	σ*	1.60814	2.95	1.27	0.055
N2-C3	σ	1.98832	C1-N10	σ*	1.98659	3.79	1.25	0.062
C3-N4	σ	1.98341	C5-N9	σ*	1.98341	8.43	1.27	0.093
C3-N4	σ	1.98307	C1-N2	σ*	1.71529	8.41	0.30	0.047
			C5-C6	σ*	1.97113	28.28	0.32	0.090

C3-H16	σ	1.98040	C1-N2	σ^*	1.98209	5.11	1.03	0.065
	σ		N4-C5	σ^*	1.98307	4.42	1.05	0.061
N4-C5	σ	1.98307	C5-C6	σ^*	1.97113	3.00	1.39	0.058
C5-C6	σ	1.97113	C1-C6	σ^*	1.97616	3.50	1.25	0.059
	σ		C1-N10	σ^*	1.98659	4.96	1.15	0.067
	σ		N9-H18	σ^*	1.98977	4.31	1.15	0.063
C5-C6	σ	1.60814	C1-N2	σ^*	1.98209	31.18	0.27	0.082
	σ		C3-N4	σ^*	1.98341	11.78	0.27	0.051
	σ		N7-C8	σ^*	1.98455	16.53	0.27	0.060
C5-N9	σ	1.98439	C1-C6	σ^*	1.97616	3.24	1.37	0.060
C6-N7	σ	1.97603	N4-C5	σ^*	1.98307	3.96	1.30	0.064
	σ		C8-H17	σ^*	1.98522	5.02	1.23	0.070
N7-C8	σ	1.98455	C1-C6	σ^*	1.97616	6.28	1.38	0.084
N7-C8	σ	1.88893	C5-C6	σ^*	1.60814	16.75	0.34	0.074
	σ		N4-C5	σ^*	1.98307	5.60	1.35	0.078
C8-H17	σ	1.98887	C5-N9	σ^*	1.98439	2.96	1.04	0.050
	σ		C6-N7	σ^*	1.97603	3.30	1.05	0.053
N10-H19	σ	1.97906	C1-C6	σ^*	1.97616	6.27	1.15	0.076
C11-C12	σ	1.98234	C12-C13	σ^*	1.93773	3.04	1.30	0.056
	σ		C13-C15	σ^*	1.98072	3.37	1.05	0.053
C12-C13	σ	1.93773	N10-C11	σ^*	1.97030	4.22	0.60	0.045
	σ		C15-H27	σ^*	1.98221	2.90	0.70	0.041
C12-H22	σ	1.97326	C11-H20	σ^*	1.98017	2.48	0.93	0.043
	σ		C13-C14	σ^*	1.98327	7.32	0.92	0.073
C13-C14	σ	1.98327	C12-C13	σ^*	1.93773	2.95	1.30	0.055
	σ		C12-H22	σ^*	1.97326	2.32	1.12	0.046
C13-C15	σ	1.98072	C11-C12	σ^*	1.98324	4.67	1.05	0.062
	σ		C12-C13	σ^*	1.98155	2.91	1.29	0.055
C14-H23	σ	1.98896	C13-C15	σ^*	1.98072	3.55	0.93	0.051
C14-H24	σ	1.97995	C12-C13	σ^*	1.98155	3.71	0.57	0.042
C14-H25	σ	1.98114	C12-C13	σ^*	1.93773	3.64	0.57	0.041
C15-H26	σ	1.99013	C13-C14	σ^*	1.98327	3.61	0.93	0.052
C15-H27	σ	1.98221	C12-C13	σ^*	1.93773	3.47	0.57	0.040
N2	LP	1.99942	C1-C6	σ^*	1.97616	9.90	0.89	0.085
	LP		C3-N4	σ^*	1.98341	12.30	0.86	0.093
N4	LP	1.99942	N2-C3	σ^*	1.98832	11.31	0.88	0.090
	LP		C5-C6	σ^*	1.97113	11.19	0.92	0.091
N7	LP	1.99945	C8-N9	σ^*	1.98887	8.77	0.81	0.076
N9	LP	1.99931	C5-C6	σ^*	1.59819	39.84	0.30	0.099
	LP		N7-C8	σ^*	1.98455	47.23	0.28	0.104
N10	LP	1.81614	C1-N2	σ^*	1.98209	22.59	0.30	0.078
C1-N2	σ^*	0.02347	C5-C6	σ^*	1.71529	157.51	0.02	0.083
C3-N4	σ^*	0.02873	C5-C6	σ^*	1.98341	130.55	0.02	0.075
N7-C8	σ^*	0.00792	C5-C6	σ^*	1.98455	61.80	0.03	0.057

interaction in molecular systems. The second order Fock matrix was carried out to evaluate the donor-acceptor interactions in the NBO analysis [26]. Some electron donor orbital, acceptor orbital and the interacting stabilization energy resulting from the second-order micro disturbance theory is reported [27,28]. The result of interaction is a loss of occupancy from the concentration of electron NBO of the idealized Lewis structure into an empty non-Lewis orbital. For each donor (i) and acceptor (j), the stabilization energy $E^{(2)}$ associated with the delocalization $i \rightarrow j$ is estimated as

$$E(2) = -n_{\sigma} \frac{\langle \sigma | F | \sigma \rangle^2}{\epsilon_{\sigma}^* - \epsilon_{\sigma}} = -n_{\sigma} \frac{F_{ij}^2}{\Delta E} \quad (2)$$

Where, $\langle \sigma | F | \sigma \rangle^2$ or F_{ij}^2 is the Fock matrix element i and j NBO orbitals, ϵ_{σ}^* and ϵ_{σ} are the energies of σ and σ^* NBOs and n_{σ} is the population of the donor σ orbital. The larger is the $E^{(2)}$ value, the more intensive is the interaction between electron donors and electron acceptors, i.e. the more donating tendency from electron donors to electron acceptors and the greater the extent of conjugation of the whole system. Delocalization of electron density between occupied Lewis type (bond or lone pair) NBO orbitals and formally unoccupied (antibonding and Rydberg) non-Lewis NBO orbitals correspond to a stabilizing donor–acceptor interaction. The NBO analysis has been performed on the compound using using NBO 3.1 program as implemented in the Gaussian 09W package at the D -B3LYP/6-31G(d,p) level of theory in order to elucidate the intramolecular interaction, rehybridization and delocalization of electron density within the molecule, which are presented in Table 4. The intramolecular hyperconjugative interactions are formed by the orbital overlap between $\sigma(\text{C-C}) \rightarrow \sigma^*(\text{C-C})$, $\pi(\text{C-C}) \rightarrow \pi^*(\text{C-C})$ which results in ICT (Intra molecular charge transfer) causing stabilization of the system. These interactions are observed as increase in electron density (ED) in C–C antibonding orbital that weakens the respective bonds. The most important interactions in the heterocyclic molecule having lone pair N(2) with that of anti bonding C1-C6 and C3–N4, results the stabilization of 9.90 and 12.30 kJ/mol. respectively. The interaction between lone pair N (4) with antibonding N2-C3 and C5–C6 resulting stabilization energy 11.31 and 11.19 kJ/mol which denotes very small delocalization. In the substitution, least energy transfer occurs from LPN7 to C5-C6(6.71kJ/mol) and C8-N9(8.77). The interaction between lone pair N9 with antibonding C5-C6 and C8-N9 resulting stabilization energy 39.84 and 47.23 kJ/mol which denotes larger delocalization. The maximum energy transfer occurs from $\sigma^*(\text{C1-N2})$ to $\sigma^*(\text{C5-C6})$ and $\sigma^*(\text{C3-N4})$ to $\sigma^*(\text{C5-C6})$ (157.51 and 130.55kJ/Mol), respectively as listed in Table 4.

5. HOMO, LUMO energy gap:

The conjugated molecules are characterized by a small highest occupied molecular orbital–lowest unoccupied molecular orbital (HOMO–LUMO) separation, which is the result of a significant degree of intra-molecular charge transfer (ICT) from the end-capping electron-donor groups to the efficient electron-acceptor groups through π -conjugated path. The strong charge transfer interaction through π -conjugated bridge results in substantial ground state donor–acceptor mixing and the appearance of a charge transfer band in the electronic absorption spectrum. Consequently, an ED transfer occurs from the more aromatic part of the π -conjugated

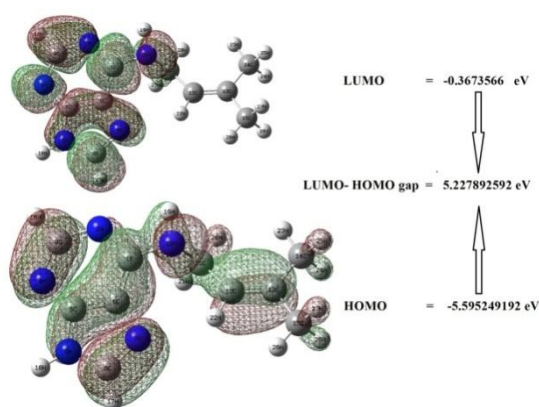


Fig.5: Visualization of the molecular orbitals of 6-(Y,Y-Dimethylallylamino)purine {HOMO—MO:54 and LUMO—MO:55}.

system in the electron donor side to its electron-withdrawing part mainly of quinonoid form. Furthermore, the HOMO and LUMO topologies show certain overlap of two orbitals in the middle region of the π -conjugated systems, The HOMO represents the ability to donate an electron, LUMO as an electron acceptor represents the ability to obtain an electron. The HOMO and LUMO energy and some other parameters calculated by B3LYP/6-31G(d,p) method are given in table 5.

Table 5: The calculated quantum chemical parameters for 6-(Y,Y-Dimethylallylamino)purine obtained by B3LYP/6-31 G(d,p) calculations

Property	6-(Y,Y-Dimethylallylamino)purine
Total energy (eV)	-17918.766
E_{HOMO} (eV)	-5.9952597
E_{LUMO} (eV)	-0.9246501
$E_{\text{HOMO}}-E_{\text{LUMO}}$ (eV)	-5.0706096
Electronegativity (χ)eV	3.4599549
Chemical hardness(η)eV	-2.5353048
Electrofilicity index (ω) eV	-2.3609169
Global Softness (σ)eV	-0.3944298
Total energy change(ΔE_T) eV	0.6338262
Dipole moment(D)	2.5327

The HOMO and LUMO gap has been calculated to be 5.227892592eV. Hence this molecule can be used as a potential source for UV light. The HOMO and LUMO energy gap explains the eventual charge transfer interactions taking place within the molecule. Moreover, these orbital significantly overlap in their position for the compound (Fig. 5). The frontier orbital gap helps characterize the chemical reactivity and kinetic stability of the molecule. A molecule with a small frontier orbital gap is more polarizable and is generally associated with a high chemical reactivity, low kinetic stability and is also termed as soft molecule. The dipole moment in a molecule is another important electronic property that results from non-uniform distribution of charges on the various atoms in a molecule. It is mainly used to study the intermolecular interactions involving the Van der Waal type dipole-dipole forces, etc., because larger the dipole moment, stronger will be the intermolecular interactions. The calculated dipole moment value for the molecule is 2.5327 Debye (Table 5) which indicates that the compound exhibits more molecular interactions.

6. UV-Visible spectrum analysis:

Ultraviolet spectra analyses of 6DMP have been investigated by SAC-CI method. The calculated visible absorption maxima of λ_{max} which are a function of the electron availability have been reported in Table 6 and Fig. 6. Calculations of molecular orbital geometry show that the visible absorption maxima of this molecule correspond to the electron transition between frontier orbitals such as transition from HOMO to LUMO. As can be seen from the UV-vis spectra absorption maxima values have been found to be 173.09 nm. The λ_{max} is a function of substitution, the stronger the donor character of the substitution, the more electrons pushed into the molecule,

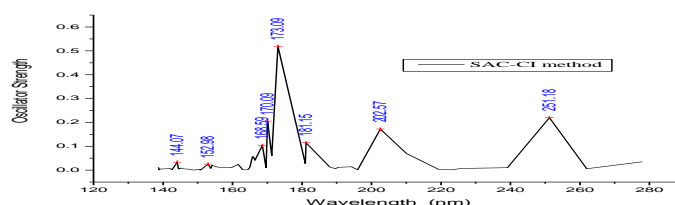


Fig.6: Theoretical UV/Vis spectrum of 6-(Y,Y-Dimethylallylamino)purine

Table 6: The UV-vis excitation energy and oscillator strength for 6DMP calculated by SAC-CI method.

No.	Energy (cm-1)	Wavelength (nm)	Osc. Strength	Symmetry	Major contribs
1	35974.99	277.97	0.0349	Singlet-A	H-2->LUMO (10%), HOMO->LUMO (84%)
2	38177.71	261.93	0.006	Singlet-A	H-2->LUMO (71%), H-1->LUMO (-22%)
3	39812.60	251.17	0.2199	Singlet-A	H-2->LUMO (14%), H-1->LUMO (68%), HOMO->LUMO (-11%)
4	41814.49	239.15	0.0103	Singlet-A	H-3->LUMO (22%), H-1->L+1 (-21%), HOMO->L+1 (50%)
5	44277.72	225.84	0.0072	Singlet-A	H-3->LUMO (-12%), H-2->L+1 (43%), H-1->L+1 (21%), HOMO->L+1 (20%)
6	44854.41	222.94	0.0011	Singlet-A	H-5->LUMO (-29%), H-4->LUMO (66%)
7	45601.28	219.29	0.0029	Singlet-A	H-2->L+1 (48%), H-1->L+1 (-24%), HOMO->L+1 (-24%)
8	47608.81	210.04	0.0695	Singlet-A	H-5->LUMO (41%), H-4->LUMO (15%), H-3->LUMO (27%)
9	49366.31	202.56	0.1721	Singlet-A	H-5->LUMO (-22%), H-4->LUMO (-10%), H-3->LUMO (23%), H-1->L+1 (22%)
10	51010.88	196.03	0.0013	Singlet-A	HOMO->L+2 (80%) H-1->L+2 (-3%), HOMO->L+3 (-7%)
11	51492.40	194.20	0.0141	Singlet-A	H-1->L+2 (-11%), H-1->L+3 (-37%), HOMO->L+3 (47%)
12	52519.15	190.40	0.0118	Singlet-A	H-6->LUMO (19%), H-5->L+1 (-25%), H-4->L+1 (48%)
13	52736.92	189.62	0.0064	Singlet-A	H-6->LUMO (52%), H-4->L+1 (-12%)
14	53191.01	188.00	0.0129	Singlet-A	H-1->L+2 (72%), H-1->L+3 (-17%), H-6->LUMO (-3%), HOMO->L+2 (2%)
15	55202.57	181.15	0.1146	Singlet-A	H-5->L+1 (10%), H-3->L+1 (53%), H-2->L+2 (10%)
16	55266.29	180.94	0.0273	Singlet-A	H-6->LUMO (12%), H-3->L+1 (-10%), H-2->L+2 (56%)
17	57774.69	173.08	0.5192	Singlet-A	H-2->L+3 (13%), H-1->L+3 (29%), HOMO->L+3 (22%) H-7->LUMO (4%), H-5->L+1 (-7%), H-4->L+1 (-3%), H-3->L+1 (2%), H-1->L+2 (5%), HOMO->L+2 (5%), HOMO->L+5 (3%)
18	58368.32	171.32	0.0604	Singlet-A	H-7->LUMO (57%), H-2->L+3 (-11%)
19	58791.77	170.09	0.2052	Singlet-A	H-5->L+1 (34%), H-4->L+1 (16%), H-3->L+1 (-11%), H-2->L+3 (12%) H-3->LUMO (3%), H-3->L+2 (-4%), H-3->L+3 (2%), H-1->L+3 (2%), HOMO->L+3 (2%)
20	58936.14	169.67	0.0098	Singlet-A	H-1->L+4 (-24%), HOMO->L+4 (58%)
21	59314.42	168.59	0.1037	Singlet-A	H-2->L+3 (40%) H-8->LUMO (6%), H-7->LUMO (8%), H-3->L+2 (6%), H-2->L+2 (8%),

					H-1->L+3 (-5%), H-1->L+4 (-5%), HOMO->L+2 (-2%), HOMO->L+3 (-9%), HOMO->L+5 (-2%)
22	60062.91	166.49	0.0413	Singlet-A	H-8->LUMO (-13%), H-6->L+1 (48%)
23	60230.67	166.02	0.0555	Singlet-A	HOMO->L+5 (57%)H-8->LUMO (9%), H-6->L+1 (9%), H-3->L+2 (4%), H-1->L+4 (8%)
24	60321.81	165.77	0.0566	Singlet-A	H-6->L+1 (-16%), H-3->L+2 (58%),H-8->L+1 (3%), H-4->L+1 (2%), H-3->L+3 (-3%), H-2->L+3 (-2%)
25	60614.59	164.97	0.0115	Singlet-A	H-8->LUMO (51%), HOMO->L+5 (-13%)
26	60833.17	164.38	0.0016	Singlet-A	H-5->L+2 (-23%), H-4->L+2 (43%),H-8->LUMO (-5%), H-6->L+1 (5%), H-5->L+3 (5%), H-4->L+3 (-5%), H-3->L+2 (5%)
27	61355.82	162.98	0.0012	Singlet-A	H-3->L+3 (79%) H-5->L+2 (3%), H-5->L+3 (3%), H-4->L+3 (2%), H-3->L+2 (4%), H-2->L+3 (-2%)
28	61872.02	161.62	0.0238	Singlet-A	H-1->L+4 (40%), H-1->L+5 (20%), HOMO->L+4 (26%) HOMO->L+5 (-3%), HOMO->L+6 (-3%)
29	62632.61	159.66	0.01	Singlet-A	H-1->L+4 (-16%), H-1->L+5 (61%),HOMO->L+4 (-9%), HOMO->L+5 (3%), HOMO->L+6 (-4%)
30	64162.65	155.85	0.012	Singlet-A	H-4->L+2 (17%), H-4->L+3 (63%),H-7->L+3 (-2%), H-6->L+3 (-3%), H-5->L+2 (2%), H-3->L+3 (-5%)
31	64774.02	154.38	0.0185	Singlet-A	H-5->L+2 (43%), H-5->L+3 (12%), H-4->L+3 (-11%) H-9->LUMO (6%), H-8->L+1 (-2%), H-7->L+1 (3%), H-4->L+2 (6%), H-3->L+3 (-3%), HOMO->L+6 (3%)
32	64903.88	154.07	0.02	Singlet-A	H-1->L+6 (14%), HOMO->L+6 (69%)H-5->L+3 (-8%), H-1->L+5 (3%)
33	65037.77	153.75	0.0075	Singlet-A	H-5->L+3 (36%), H-2->L+4 (39%),H-9->LUMO (-5%), H-4->L+2 (-2%), HOMO->L+6 (3%)
34	65366.04	152.98	0.0253	Singlet-A	H-5->L+3 (-23%), H-2->L+4 (54%) H-9->LUMO (7%), H-4->L+2 (4%)
35	66316.97	150.79	0.0001	Singlet-A	H-7->L+1 (74%) H-6->L+1 (7%), H-5->L+2 (-5%), H-4->L+2 (-4%)
36	66430.70	150.53	0.0034	Singlet-A	H-10->LUMO (14%), H-9->LUMO (67%)
37	67109.82	149.00	0.0002	Singlet-A	H-10->LUMO (73%), H-9->LUMO (-10%)
38	67513.91	148.11	0.0019	Singlet-A	H-3->L+4 (83%) H-5->L+4 (-7%), H-4->L+4 (-6%)
39	67882.50	147.31	0.0044	Singlet-A	H-8->L+1 (71%) H-13->LUMO (-2%), H-11->LUMO (-4%), H-10->LUMO (-3%), H-6->L+1 (3%), H-4->L+3 (-3%)
40	68497.91	145.98	0.005	Singlet-A	H-8->L+3 (11%), H-7->L+3 (23%), H-6->L+2 (17%), H-6->L+3 (19%)H-8->L+1 (7%), H-8-

41	68913.29	145.10	0.0084	Singlet-A	>L+2 (2%), H-7->L+2 (4%), H-4->L+3 (6%) H-6->L+2 (20%), H-1->L+6 (46%) H-11->LUMO (-7%), H-6->L+3 (-3%), HOMO->L+6 (-6%), HOMO->L+8 (6%)
42	69193.97	144.52	0.0043	Singlet-A	H-6->L+2 (33%), H-6->L+3 (-17%), H-2->L+5 (10%), H-1->L+6 (-19%) H-8->L+2 (-3%), H-7->L+2 (-5%), HOMO->L+6 (3%), HOMO->L+8 (-2%)
43	69235.11	144.43	0.0068	Singlet-A	H-11->LUMO (-15%), H-2->L+5 (59%)
44	69409.32	144.07	0.0332	Singlet-A	H-11->LUMO (56%), H-2->L+5 (18%)
45	70119.10	142.61	0.0021	Singlet-A	H-1->L+7 (-20%), HOMO->L+7 (54%), HOMO->L+8 (-16%)
46	70440.11	141.96	0.007	Singlet-A	HOMO->L+7 (12%), HOMO->L+8 (63%)
47	70769.99	141.30	0.006	Singlet-A	H-5->L+4 (46%), H-4->L+4 (27%), H-3->L+4 (12%), H-3->L+5 (5%)
48	71840.29	139.19	0.0045	Singlet-A	H-5->L+4 (-14%), H-3->L+5 (68%), H-3->L+6 (2%), HOMO->L+7 (-2%)
49	72006.45	138.87	0.0009	Singlet-A	H-7->L+2 (-14%), H-5->L+4 (-10%), H-4->L+4 (32%)
50	72112.10	138.67	0.0116	Singlet-A	H-8->L+3 (-11%), H-7->L+3 (22%), H-5->L+4 (-11%), H-4->L+4 (17%)

the larger λ_{\max} . These values may be slightly shifted by solvent effects. The role of substituent and of the solvent influence on the UV-spectrum. Owing to the interaction between HOMO and LUMO orbital of a structure, transition state transition of π - π^* type is observed with regard to the molecular orbital theory [29].

6. NLO Properties:

The second-order polarizability or first hyperpolarizability β , dipole moment μ and polarizability α was calculated using HF/6-31G(d,p) basis set on the basis of the finite-field approach. The complete equations for calculating the magnitude of total static dipole moment μ , the mean polarizability α_0 , the anisotropy of the polarizability $\Delta\alpha$ and the mean first hyperpolarizability β_0 , using the x, y, z components from Gaussian 09W output is as follow

$$\mu = \mu_x^2 + \mu_y^2 + \mu_z^2 \quad (3)$$

$$\alpha_0 = \frac{\alpha_{xx} + \alpha_{yy} + \alpha_{zz}}{3} \quad (4)$$

$$\Delta\alpha = 2^{-1/2} [(\alpha_{xx} - \alpha_{yy})^2 + (\alpha_{yy} - \alpha_{zz})^2 + 6\alpha_{xx}^2]^{1/2} \quad (5)$$

$$\beta = (\beta_x^2 + \beta_y^2 + \beta_z^2)^{1/2} \quad (6)$$

and

$$\beta_x = \beta_{xxx} + \beta_{xyy} + \beta_{xzz} \quad (7)$$

$$\beta_y = \beta_{yyy} + \beta_{xxy} + \beta_{yzz} \quad (8)$$

$$\beta_z = \beta_{zzz} + \beta_{xxz} + \beta_{yyz} \quad (9)$$

Since the values of the polarizabilities (α) and hyperpolarizability (β) of Gaussian 09W output are reported in atomic units (a.u), the calculated values have been converted into electrostatic units (esu) (α : 1 a.u = 0.1482 x 10⁻¹² esu, β : 1 a.u = 8.6393 x 10⁻³³ esu). The total first hyperpolarizability of the title compound has been calculated

to be 6.425×10^{-30} esu as shown in Table 7. This result shows that the compound is one of the best materials for NLO applications.

Table 7: Calculated all β components and β_{tot} value of 6-(Y,Y-Dimethylallylamino)purine by HF/6-31G (d, p) method

6-(Y,Y-Dimethylallylamino)purine	
β_{xxx}	93.944589
β_{xxy}	16.878853
β_{xyy}	-32.4701738
B_{yyy}	-41.0556007
β_{xxz}	-87.3647925
β_{xyz}	-3.8567031
B_{yyz}	-48.2320262
β_{xzz}	16.1641093
β_{yzz}	-30.4840093
β_{zzz}	5.5381738
$\beta_{\text{total}} \text{ (esu)}$	6.425×10^{-30} esu

7. Thermodynamic properties

On the basis of vibrational analyses and statistical thermodynamics, the standard thermodynamic functions: heat capacity, internal energy, entropy and enthalpy were calculated using Moltranv.2.5[30] and are listed in supplementary material. As observed from Table 8, the values of C_p , C_v , U,H and S all increase with the increase of temperature from 10 to 500 K, which is attributed to the enhancement of the molecular vibration as the temperature increases. The correlation equations between these thermodynamic properties and temperatures were fitted by quadratic, linear and quadratic formulas, respectively, and

Table 8: Thermodynamic properties for 6-(Y,Y-Dimethylallylamino)purine obtained by B3LYP/6-31 G (d, p) density functional calculations

Temperature (K)	C_v (J/K/mol)	C_p (J/K/mol)	U (kJ/mol)	H (kJ/mol)	S (J/K/mol)	G (kJ/mol)
50.000	58.323	66.637	607.468	607.884	285.550	593.606
100.000	90.081	98.395	611.185	612.017	341.580	577.859
150.000	120.685	129.000	616.454	617.701	387.256	559.612
200.000	152.087	160.401	623.268	624.931	428.640	539.203
250.000	184.627	192.941	631.682	633.760	467.909	516.783
300.000	217.795	226.110	641.742	644.236	506.016	492.431
350.000	250.585	258.900	653.455	656.365	543.345	466.194
400.000	281.983	290.298	666.777	670.102	579.986	438.108
450.000	311.296	319.611	681.618	685.360	615.893	408.208
500.000	338.207	346.521	697.866	702.023	650.982	376.532

the corresponding fitting equations are also listed in supplementary material and the corresponding fitting factors are all beyond 0.999. All the thermodynamic data provide helpful information to further study on the title compounds. They compute the other thermodynamic energies according to relationships of thermodynamic functions and estimate directions of chemical reactions according to the second law of thermodynamics in thermochemical field.

8. Molecular electrostatic potential maps

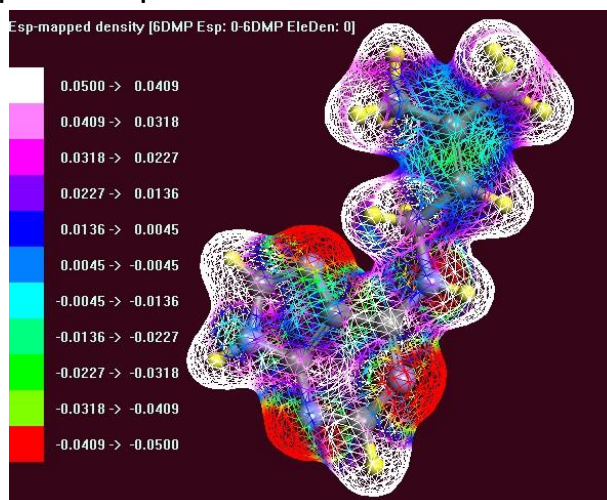


Fig. 7: B3LYP/6-31G(d, p) calculated 3D molecular electrostatic potential maps for 6-(Y,Y-Dimethylallyl amino) purine

The molecular electrostatic potential (MESP) is widely used as a reactivity map displaying most probable regions for the electrophilic attack of charged point-like reagents on organic molecules[31,32]. The molecular electrostatic potential (MESP) $V(r)$ at a point r due to a molecular system with nuclear charges $\{Z_A\}$ located at $\{R_A\}$ and the electron density $\rho(r)$ is given by

$$V(r) = \sum_A^N \left[\frac{Z_A}{|r-R_A|} - \int \rho(r') d^3r' / |r-r'| \right] \quad (10)$$

Where, N denotes the total number of nuclei in the molecule and the two terms refer to the bare nuclear potential and the electronic contributions, respectively. The balance of these two terms brings about the effective localization of electron-rich regions in the molecular system. The MESP topography is mapped by examining the eigen value of the Hessian matrix at the point where the gradient $V(r)$ vanishes. The electrostatic potential is a physical property of a molecule related to how a molecule is first “seen” or “felt” by another approaching species. A portion of a molecule that has a negative electrostatic potential will be susceptible to electrophilic attack - the more negative the better. It is not as straightforward to use electrostatic potentials to predict nucleophilic attack..

9. Conclusions

The Vibrational properties of 6-(Y,Y-Dimethylallylamino)purine have been investigated Theoretically by ab initio calculations using D -B3LYP at 6-31G basis set level. The Energy of the title compound has been calculated using the above mention basis sets. The theoretical values are agreement with experimental frequencies. The most optimized structural parameters of 6DMP were calculated by D /B3LYP level with 6-31 G (d, p) basis set. The maximum number of potentially active observable fundamentals of a non-linear molecule, which contains N atoms, is equal to $(3N - 6)$ i.e 78 were obtained and tabulated the modes. The stimulated characteristics values of Raman spectrum IR Values are studied. Second order perturbation theory analysis of fock matrix in NBO basis for 6-(Y,Y-Dimethylallylamino)purine is well studied. The HOMO and LUMO energy and some other parameters calculated by B3LYP/6-31G(d,p) method, The HOMO and LUMO gap has been calculated to be 5.227892592eV. The total first hyperpolarizability of the title compound has been calculated to be 6.425×10^{-30} esu. On the basis of vibrational analyses and statistical thermodynamics, the standard thermodynamic functions: heat capacity, internal energy, entropy and enthalpy were calculated using Moltran v.2.5 and are listed in table 8. The values of C_p , C_v , U , H and S all increase with the increase of temperature from 10 to 500 K , which is attributed to the enhancement of the molecular vibration as the temperature increases.

Acknowledgements

The first author A.Veeraiah is highly grateful to Science and Engineering Research Board(SERB), Department of Science and Technology (DST), New Delhi and the Management D.N.R. College Association, Bhimavaram for their financial and administrative support respectively.

References:

- [1] Acheson R M, An introduction to Chemistry of heterocyclic compounds, Third Edition, (John Wiley & Sons, New York), 1977
- [2] Paul O.P.Ts'O, Basic principles in nucleic acid Chemistry, Vol.1, (Academic Press, London),1974
- [3] Martin G T, Biological antagonism, (blackiston, New york),1961
- [4] M.Majoube, G. Vergoten and M. Henry DSM-DRECAM-SPAM, centred'Etudes de Sacalay, 91191 Gif surYvelteCedex, France].
- [5] A. Lautie and A.Novak, J.Chim. Phys.,65(1968) 1359
- [6] M.Majoube, M. Henry and G. Vergoten, J.RamanSpectrosc., 25(1994) 239
- [7] S.G. Stepanian, G.G. Sheina, E.D. Radhenko and Yu. P. Blagoi, J.Mol. Struct., 131 (1985) 333, 158(1987)275
- [8] M. Majoube, M.Henry, L. Chinsky and P.Y. Tuprin, Chem. Phys., 169(1993) 231
- [9] M. Majoube, Ph. Millie, P. Lagant and G. Vergoten, J. Raman Spectrosc., 25 (1994) 821
- [10] F. Skoog, H.Q. Hamzi, A.M. Szweykowska, N.J. Leopard, K.L.Carraway, T.Fujji, J.P. Helgeson, R.N. Loepky, Phytochemistry 6(1967) 1169
- [11] P.Cohen, Nat. Cell, Biol.4 (2002) E127, D.O. Morgan, Nat. Cell Biol.4 (2002) E127
- [12] R.I Pennel, C. Lamb, Plant cell 9 (1997) 1157
- [13] Y. Katakura, Biosci. Biotechnol.Biochem.70(2006) 1076, C.A. Schmidt, Biochim.Biophys, Acta-Rev. Cancer 1775 (2007) 5,
- [14] T.M. Sielecki, J.F. Boylan, P.A. Benfield, G.L. Trainor, J. Med. Chem. 43 (2000) 1
- [15] A.D. Becke, Phys. Rev. A 38 (1988) 3098
- [16] C. Lee, W. Yang, R.G. Parr, Phys. Rev. B 37 (1988) 785
- [17] M. J. Frisch, G. W. Trucks, H. B. Schlegel, G. E. Scuseria, M. A. Robb, J. R. Cheeseman, G. Scalmani, V. Barone, B. Mennucci, G. A. Petersson, H. Nakatsuji, M. Caricato, X. Li, H. P. Hratchian, A. F. Izmaylov, J. Bloino, G. Zheng, J. L. Sonnenberg, M. Hada, M. Ehara, K. Toyota, R. Fukuda, J. Hasegawa, M. Ishida, T. Nakajima, Y. Honda, O. Kitao, H. Nakai, T. Vreven, J. A. Montgomery, Jr., J. E. Peralta, F. Ogliaro, M. Bearpark, J. J. Heyd, E. Brothers, K. N. Kudin, V. N. Staroverov, R. Kobayashi, J. Normand, K. Raghavachari, A. Rendell, J. C. Burant, S. S. Iyengar, J. Tomasi, M. Cossi, N. Rega, J. M. Millam, M. Klene, J. E. Knox, J. B. Cross, V. Bakken, C. Adamo, J. Jaramillo, R. Gomperts, R. E. Stratmann, O. Yazyev, A. J. Austin, R. Cammi, C. Pomelli, J. W. Ochterski, R. L. Martin, K. Morokuma, V. G. Zakrzewski, G. A. Voth, P. Salvador, J. J. Dannenberg, S. Dapprich, A. D. Daniels, Ö. Farkas, J. B. Foresman, J. V. Ortiz, J. Cioslowski, and D. J. Fox, Gaussian 09W, Revision D.01, Gaussian, Inc., Wallingford CT, 2009
- [18] A. Frisch, A. B. Nielsen, A. J. Holder, GaussviewUsers Manual Gaussian Inc., Pittsburg
- [19] www.chemcra.org.
- [20] P. Pulay, G. Fogarasi, F. Pang, and J. E. Boggs, J. Am. Chem. Soc. 101 (1979) 2550
- [21] G. Fogarasi, X. Zhou, P.W. Taylor, P. Pulay, J. Am. Chem. Soc. 114 (1992) 8191
- [22] E.D. Glendering, A.E. Reed, J.E. Carpenter, F. Weinhold, NBO version 3.1, TCI, University of Wisconsin, Madison, 1998.
- [23] M. Silverstein, G. Clayton Bassler, C. Morrill, Spectroscopic Identification of Organic Compounds, John Wiley, New York, 1981,
- [24] E.B. Wilson, J.C. Decius, P.C. Cross, Molecular Vibrations, Dover Publ. Inc., New York, 1980

- [25] P. Pulay, G. Fogarasi, F. Pang, and J. E. Boggs , J. Am. Chem. Soc. 101 (1979) 2550, G. Fogarasi, X. Zhou, P.W. Taylor, P. Pulay, J. Am. Chem. Soc. 114 (1992) 8191
- [26] M. Sarafran, A. Komasa, E.B. Adamska, J. Mol. Struct. (Theochem.)827 (2007)101
- [27]C. James, A. AmalRaj, R. Reghunathan, I. Hubert Joe, V.S. JayaKumar, J. Raman Spectrosc. 37 (2006) 1381,
- [28] L.J. Na, C.Z. Rang, Y.S. Fang, J. Zhejiang Univ. Sci. 6B (2005) 584
- [29] G. Gece, Corros. Sci. 50 (2008) 2981, K. Fukui, Theory of Orientation and Stereoselection, Springer-Verlag, Berlin, 1975, K.Fukui, Science 218 (1987) 747
- [30] S.K. Ignatov, Moltran v.2.5 - Program for molecular visualization and thermodynamic
- [31]P. Politzer, D.G. Truhlar (Eds.), Chemical Application of Atomic and Molecular Electrostatic Potentials, Plenum, New York, 1981
- [32]P. Politzer and J. S. Murray, Rev. Comp. Chem., 2 VCH (1991) 273